Upper Airway Segmentation using Fast Marching

César Bustacara-Medina
Pontificia Universidad Javeriana
Bogotá D.C., Colombia
cbustaca@javeriana.edu.co

Leonardo Flórez-Valencia
Pontificia Universidad Javeriana
Bogotá D.C., Colombia
florez-l@javeriana.edu.co

José Hernando Hurtado
Pontificia Universidad Javeriana
Bogotá D.C., Colombia
hhurtado@javeriana.edu.co

ABSTRACT

Direct measurements of airway tree and wall areas are potentially useful as a diagnostic tool and as an aid to understanding pathophysiology underlying of the airway diseases. Direct measurements can be made from images obtained using computer tomography (CT) by applying computer-based algorithms to segment airway, however, current validation techniques cannot establish adequately the accuracy of these algorithms. Additional, the majority of the studies only include the airway from trachea to bronchi's tree avoiding the upper respiratory system, because the main problems appears in the lower respiratory system, for example, asthma and chronic obstructive pulmonary (airflow obstruction or limitation, including chronic bronchitis, emphysema and bronchiectasis). Airway tree segmentation can be performed manually by an image analyst, but the complexity of the tree makes manual segmentation tedious and extremely time-consuming (require several hours of analysis), only including trachea and lower airway system. Airway segmentation in CT images is a challenging problem for two reasons, it is a complex anatomy and exists limitations in image quality inherent to CT image acquisition. This paper describes a semi-automatic technique to segment the airway tree (upper airway system and trachea), using CT images of head-neck and applying a fast marching algorithm. Additionally, a heuristic is proposed to determine the algorithm parameters without have to review manually all structures to segmentation.

Keywords

Image segmentation, Airway tree, Fast marching, Computed tomography.

1.   INTRODUCTION

Image analysis techniques have been broadly used in computer-aided medical analysis and diagnosis in recent years [3][4][5][6][7]. Computer-aided image analysis is an increasingly popular tool in medical research and practice, especially with the increase of medical images in modality, amount, size, and dimension. Image segmentation, a process that aims at identifying and separating regions of interests from an image, is crucial in many medical applications such as localizing pathological regions, providing objective quantitative assessment and monitoring of the onset and progression of the diseases, as well as analysis of anatomical structures [8][9][10][11][12]. A number of techniques have been developed for segmenting and analyzing the 3-D airway tree. Kitasaki *et al.* [13] used a voxel classification based on local intensity structure. Hirano *et al.*[14] used the cavity enhancement filter and the region-growing method. Park *et al.* developed an integrated software package utilizing a new measurement algorithm called mirror-image Gaussian fit (MIGF), that enables the user to perform automated bronchial segmentation, and measurement. In addition, MIGF permits to delineate the outer wall of bronchia. Bauer [16] used Gradient Vector Flow (GVF) method to produces accurate segmentation of the airway lumen. Aykac et *al.* [1] used grayscale morphological reconstruction to identify candidate airways. Park et *al.* [17] used 3-D confidence connected region growing (CCRG) method to extract lower and upper airways of the bronchi.

Many researchers agree that the complex branching structure of the human airway tree can be examined using computed tomography (CT) imaging. Quantitative analyses can be performed on the three-dimensional (3D) airway tree to evaluate tree structure and function [2][18][14][15][17]. It is important to note that most of segmentations are performed of the trachea and the lower airway tree, but in our case, the segmentation of the upper airway and trachea is necessary, since the results will be used to characterize the possible causes of sleep apnea in a series of 387

patients.

In this paper we will use the level sets technique proposed for Osher and Sethian in 1988 [19], specifically, the fast marching method introduced by Sethian in 1995 [20][21]. As shown by Sethian, fast marching is a set of finite difference numerical techniques that were constructed to solve the Eikonal equation, which is a boundary value partial differential equation. These techniques rely on a marriage between the numerical technology for computing the solution to hyperbolic conservation laws and the causality relationships inherent in finite difference upwind schemes. Fast marching methods are Dijkstra type methods, in that they are closely connected to Dijkstra's well-known network path algorithms [22].

2.   MATERIALS

Our proposed method has been applied to 70 patients. By each patient, two CT scan were acquired, one in awake and other in induced sleep. The dataset include the head and thorax, because we are interested in the upper airway and the trachea, specifically, from the lower trachea to the nasal conchae as illustrated in Fig. 1. The paranasal sinus region contains several membrane-like structures, affected by partial volume effects, which renders the segmentation as a non-trivial process. Additionally, poor contrasts are usually caused by existing metal parts (tooth implants or other implants) that appear in extremely high intensities relative to the actual anatomical structures. The image size of all patients dataset is 512×512 pixels in each slice, 460 - 840 slices per image, 0.368-0.586 [mm] in pixel spacing, and 0.299-0.301[mm] in slice spacing, respectively.
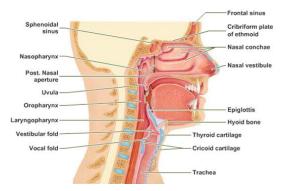

Fig. 1 Upper Airway Anatomy, adapted from [23]

The fast marching segmentation method is implemented in the Insight Segmentation and Registration Toolkit (ITK) and can be downloaded from www.itk.org [24]. ITK was funded by the National Library of Medicine (NLM), and it is open-source software that was developed jointly by six principal organizations to support the Visible Human project of NLM. ITK includes several basic segmentation and registration techniques that have been implemented for a variety of medical image analysis applications. Additionally, the visualization was made using the Visualization Toolkit (VTK).

3.   METHOD

Fast marching methods are finite difference techniques, more recently extended to unstructured meshes, for solving the Eikonal equation of the form[21]:

$$|\nabla T| F(x, y, z) = 1, T = 0 \text{ on } \Gamma \qquad (1)$$

This can be thought of as a front propagation problem for a front initially located at Γ and propagating with speed $F(x, y, z,) > 0$. The evolution of the function is controlled by a partial differential equation in which a speed term F is involved. In our case, we use the fast marching filter implemented in ITK as illustrated in Fig. 2.
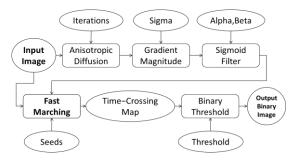

Fig. 2 Fast marching algorithm in ITK

A typical speed image is produced by mapping of gradient magnitude of the original image. The mapping is selected in such a way that regions with high contrast will have low speeds while homogeneous regions will have high speed. In this case the mapping of gradient magnitude is made with a sigmoid function. The fast marching filter will propagate a front starting from the seed points defined for the user and traveling with the speed computed from the speed image. This should result in the contour slowing down close to object edges. The result of the filter is a time-crossing map which indicates for each pixel, how long it took to the contour to reach this pixel.

3.1   Gradient magnitude

Obtaining a good gradient magnitude is important to define the limits of the structures that you want to segment and thus be able to apply a sigmoid filter to obtain the speed function that the fast-marching algorithm will use. According to the above, it is necessary to determine the most appropriate algorithm and parameters to obtain the maximum gradient

magnitude. These algorithms are associated with edge detection achieving as indicated by Canny and Deriche [25][26], applying an efficient criterion for edge detection, which allows a good detection, localization and good response to a single edge.

The good detection implies that there must be a very low probability of failure in detecting a real edge at some point and a low probability of scoring points that are not edges. This criterion as indicated by Canny [25], corresponding to maximize the signal-noise ratio (SNR), which means, find the maximum response of the detection criterion, which correspond to find the best operator to detect edges only.

To detect sudden intensity changes in the image two approaches have been used. The first, location of the extremes (maxima and minima) of the first derivative of the intensity function (image), and the second, location of the zero crossings or transitions from negative to positive values, or vice versa, from the second derivative of the intensity function (image). Besides these detectors based on the gradient or Laplacian, others have been proposed by optimizing certain criteria related with edge detection, the most popular algorithms are the Canny [25][27] and Deriche [26].

In this case, Deriche's algorithm which is based on the Canny will be used because proposes a robust formulation for the detection and location. In addition, using the Deriche-filter leads to a distortion of the amplitudes of the edges depending on their direction. The implementation presented by ITK for Deriche filter is called "RecursiveGaussianImageFilter" [24], the base class is defined to calculate the convolution of the IIR filter with a Gaussian kernel approach

$$\frac{1}{\sigma\sqrt{2\pi}} e^{-\left(\frac{x^2}{2\sigma^2}\right)} \qquad (2)$$

This class, according to ITK documentation, implements the Deriche's recursive filter proposed in his paper [26] and details or modifications presented by Deriche [28] and Farneback *et al.* [29]. Meanwhile, the magnitude of the gradient is calculated using the filter called "GradientMagnitudeRecursiveGaussianImageFilter", which convolved with the first derivative of a Gaussian function and invokes Deriche filter. In addition, the sigma (σ) parameter according with ITK is measured in spacing units of the image.

3.2   Sigmoid function
According to documentation provided by ITK [24], the sigmoid filter is commonly used as a transformation of intensity. Through this filter, for a specific range of intensity values is generated a new

range of intensity obtaining a very smooth and continuous transition at the boundaries of the range. A sigmoid function is widely used as a mechanism to focus attention on a particular set of values and progressively reduce the values outside that range. It should be noted that this filter is a pixel operator, that is, for a given input generates a single output value.

The implementation of the sigmoid filter in ITK includes four parameters that can be adjusted to select their range of input and output intensity. Equation (3) represents the sigmoid transformation applied to each pixel of the image [24].

$$I' = (Max - Min) \cdot \frac{1}{\left(1+e^{\left(\frac{I-\beta}{\alpha}\right)}\right)} + Min \qquad (3)$$

The heuristic proposed by ITK to find the appropriate values to evaluate the sigmoid filter is: taking the image result to calculate the gradient magnitude, you must select the minimum value (K1) along the contour of the anatomical structure to be segmented. Then select the mean value (K2) of the gradient magnitude at the center of the structure. Under ideal conditions, K1 will always be greater than K2. This happens because K1 is located on the contour and K2 is located in the valley of the structure to be segmented. These two values indicate the dynamic range to be mapped to the interval [0, 1] in the resulting image, which will be used as the speed function for Fast Marching segmentation method. After other considerations, this mapping will produce a speed image such that the level set, it will march rapidly on the homogeneous region and it will stop on the contour. The suggested value for β is (K1+K2)/2 while the suggested value for α is (K2-K1)/6, which must be a negative number. In our case, determine the appropriate value for K1 is quite difficult and tedious because the target structure is elongated and presents complex regions (upper airway), requiring much time to explore the contours per-slice.
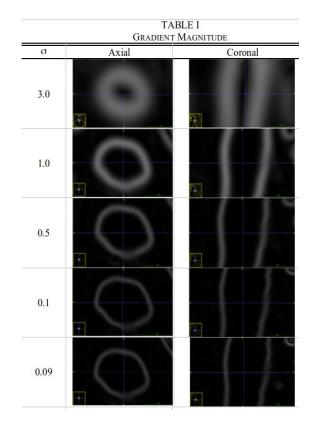
One important phase in the segmentation process is based on the adaptation (tuning) of gradient magnitude and sigmoid function parameters. The approach is based on define the parameters using visual information obtained from ideal behavior of the functions. This will reduce time-consuming due to the user-interaction required per-slice.

4.   RESULTS
Pre-processing is first performed on the image, which includes denoising the dataset using an edge-preserving smoothing filter (e.g. Anisotropic Diffusion). The use of such smoothing is preferable

since traditional blurring approaches tend to resolve thin, sharp structures that are important in our case. Then, "GradientMagnitudeRecursiveGaussianImageFilter" filter was applied to calculate the magnitude of the gradient.

As the objective is to determine the best value for sigma (σ), various tests were performed. Table I presents the results for a CT image (patient No. 1), varying the value of sigma between 3.0 and 0.01 (some intermediate results were omitted). As the value of sigma (σ) is reduced, the edges are appreciated more centered (focused) and localized, but this does not imply that they are of better quality (magnitude) to apply sigmoid filter and therefore obtain good segmentation of the desired region.

Since the maximum value of the gradient magnitude is locally obtained, the maximum and minimum values for the entire dataset (70 CT) were taken. Fig. 3 shows the behavior obtained by varying the sigma value between 3.0 and 0.01. The sigma value with which the maximum values for the gradient magnitude are obtained is 0.09, except in some cases whose maximum value is in sigma 0.1 and 0.08. These results are independent of the intensity range and spacing present in the images.
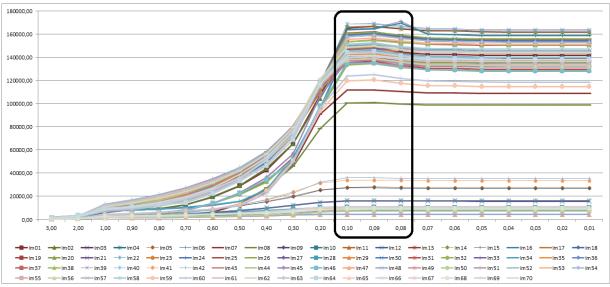

TABLE I
GRADIENT MAGNITUDE

Fig. 3 Gradient magnitudes (70 CT)

Now, verification of obtained values from the gradient magnitude images is required, for this an axial slice of the 3D image located in the area of interest (airway) is taken. Fig. 4 illustrates the analyzed region between points 213-279. Values along the x-axis are extracted and then plotted as shown in Fig. 5. The value of gradient magnitude at the edge of the analyzed region is increased as the value of sigma is decreased. The maximum value at border points (edges at 228 and 262) is reached when

sigma value is 0.09 and then remains stable.

From the above, we can conclude that the best sigma value is located between 0.1 and 0.09, so the tests of the sigmoid filter will be made with a sigma value of 0.09.

Sigmoid filter require values K1 and K2 that must be obtained from observing the gradient magnitude image. This is easier for regions to segment with certain characteristics, for example, small size and
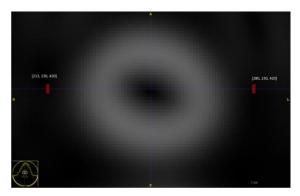
Fig. 4 Axial slice of the airways

interest was taken and the sigmoid behavior was plotted as shown in Fig. 6. To small values of K2 abrupt changes occur in the sigmoid function inside the structure. But according with the definition, it is expected that the speed function allows the propagation of level-set, thus, the speed function must go to zero smoothly on the structure boundaries, and this behavior was verified as shown in Fig. 7.

Several curves cross with x-axis, which can generate an over-segmentation (overflows the propagation front). The behavior of the sigmoid should be smooth and should not cross x-axis in the boundary of structure. Based on the above, the user can select the
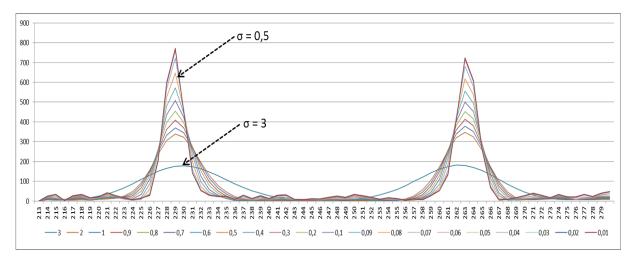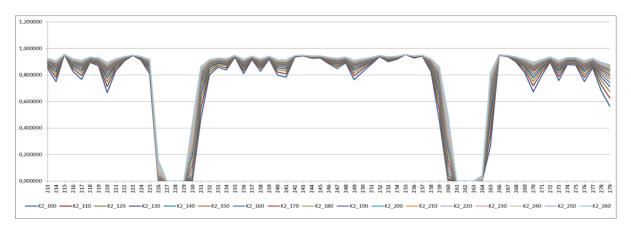

Fig. 4: Gradient magnitude in edges

Fig. 6: Sigmoid behaviors

easy navigation to extract these values accurately. But unfortunately, the above is not manageable for long structures that occupy a lot of CT slices, such as airways or blood system. The sigmoid filter was applied to the gradient magnitude images with values to K1 between 100 and 500 and K2 between 4 and 10. Just as for gradient analysis, a slice in the region of

set of curves that best satisfy the described conditions, achieving thus determine the most appropriate values for K1 and K2. In our case, the values for K1 and K2 correspond to the interval 130-160 and 6-8 respectively.
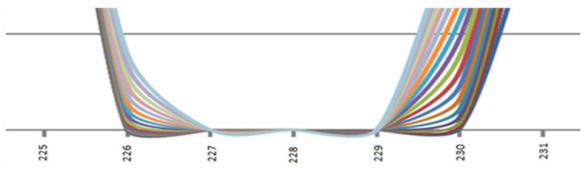
Fig. 7 Sigmoid behaviors on structure boundaries

Applying the fast marching algorithm with the parameters defined using the proposed heuristic, it is observed that as the parameter K1 is close to value 150, the results generated are closer to the real boundary of the desired structure. This imply that the proposed values are suitable for segmentation, as illustrated in Fig. 8. Further, as indicated, when the value of K1 (minimum value on the structure boundaries) is high, it is obtained an over-segmentation and vice versa a sub-segmentation.
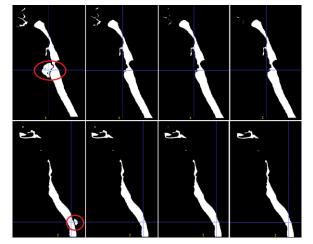

Fig. 6 Fast marching results for K1={170, 150, 140, 130} and K2=6.

With this new heuristic to determine the parameters to evaluate the gradient magnitude (K1, K2) and speed function defined for these values, the time-consuming to explore the structures to define K1 and K2 is less. This permit to eliminate the overall review of the structure to be segmented.

5.   CONCLUSIONS

We have proposed a heuristic that can be split into two main stages: Gradient magnitude and speed function. The key point of the gradient magnitude is to use optimal recursive and separable filters as Deriche proposed to obtain approximate gradient or Laplacian. Select the maximum value reduces the possibility of fronts propagation overflow outside the structures to

segment, which is associated with the second key point. The speed function can be defined using the desired behavior of sigmoid function and adjusting its values in the structure boundaries. This takes less time-consuming that search in all CT images that include part of the structure.

6.   REFERENCES

[1]   D. Aykac, E. A. Hoffman, G. McLennan, and J. M. Reinhardt, "Segmentation and analysis of the human airway tree from three-dimensional X-ray CT images.," *IEEE Trans. Med. Imaging*, vol. 22, no. 8, pp. 940–950, Aug. 2003.

[2]   W. Park, E. Hoffman, and M. Sonka, "Segmentation of intrathoracic airway trees: a fuzzy logic approach.," *IEEE Trans. Med. Imaging*, vol. 17, no. 4, pp. 489–97, Aug. 1998.

[3]   G. Székely, A. Kelemen, C. Brechbühler, and G. Gerig, "Segmentation of 2-D and 3-D objects from MRI volume data using constrained elastic deformations of flexible Fourier contour and surface models.," *Med. Image Anal.*, vol. 1, no. 1, pp. 19–34, Mar. 1996.

[4]   S. Gorthi, V. Duay, N. Houhou, M. B. Cuadra, U. Schick, M. Becker, A. S. Allal, and J. Thiran, "Segmentation of Head and Neck Lymph Node Regions for Radiotherapy Planning Using Active Contour-Based Atlas Registration," *IEEE J. Sel. Top. Signal Process.*, vol. 3, no. 1, pp. 135–147, 2009.

[5]   R. Pohle and K. D. Toennies, "Segmentation of medical images using adaptive region growing," *SPIE*, pp. 1337–1346, Jul. 2001.

[6]   J. Acharya, S. Gadhiya, and K. Raviya, "Segmentation Techniques for Image Analysis: A Review," *Int. J. Comput. Sci. Manag. Res.*, vol. 2, no. 1, pp. 1218–1221, 2013.

[7]   G. K. Seerha and R. Kaur, "Review on Recent Image Segmentation Techniques," *Int. J.*

Comput. Sci. Eng., vol. 5, no. 02, pp. 109–112, 2013.

[8] H. C. Van Assen, "3D Active Shape Modeling for Cardiac MR and CT Image Segmentation," in *3D Active Shape Modeling for Cardiac MR and CT Image Segmentation*, 2006.

[9] H. C. van Assen, M. G. Danilouchkine, M. S. Dirksen, J. H. C. Reiber, and B. P. F. Lelieveldt, "A 3-D active shape model driven by fuzzy inference: application to cardiac CT and MR.," *IEEE Trans. Inf. Technol. Biomed.*, vol. 12, no. 5, pp. 595–605, Sep. 2008.

[10] N. R. Pal and S. K. Pal, "A Review on Image Segmentation Techniques," *Pattern Recognit.*, vol. 26, no. 9, pp. 1277–1294, 1993.

[11] Z. Ma, J. M. Tavares, and R. M. Natal Jorge, "A Review on the Current Segmentation Algorithms for Medical Images," in *Proceedings of the First International Conference on Computer Imaging Theory and Applications (IMAGAPP 2009)*, 2009.

[12] S. K. Somasundaram and P. Alli, "A Review on Recent Research and Implementation Methodologies on Medical Image Segmentation," *J. Comput. Sci.*, vol. 8, no. 1, pp. 170–174, 2012.

[13] T. Kitasaka, H. Yano, M. Feuerstein, and K. Mori, "Bronchial region extraction from 3D chest CT image by voxel classification based on local intensity structure," in *Third International Workshop on Pulmonary Image Analysis*, 2010, pp. 21–29.

[14] Y. Hirano, R. Xu, R. Tachibana, and S. Kido, "A Method for Extracting Airway Trees by Using a Cavity Enhancement Filter," in *Fourth International Workshop on Pulmonary Image Analysis*, 2011, no. 21103008, pp. 91–99.

[15] R. Venkatraman, R. Raman, B. Raman, R. B. Moss, G. D. Rubin, L. H. Mathers, and T. E. Robinson, "Fully automated system for three-dimensional bronchial morphology analysis using volumetric multidetector computed tomography of the chest.," *J. Digit. Imaging*, vol. 19, no. 2, pp. 132–9, Jun. 2006.

[16] C. Bauer, "Segmentation of 3D Tubular Tree Structures in Medical Images," Graz University of Technology, Austria, 2010.

[17] S. J. Park, J. H. Kim, J. M. Goo, K. G. Kim, and S. H. Lee, "A Virtual Bronchoscopy with Color-mapped Wall Thickness," in *APAMI 2006 in conjunction with MIST 2006*, 2006, pp. 661–666.

[18] X. Zhou, T. Hayashi, T. Hara, H. Fujita, R. Yokoyama, T. Kiryu, and H. Hoshi, "Automatic segmentation and recognition of anatomical lung structures from high-resolution chest CT images.," *Comput. Med. Imaging Graph.*, vol. 30, no. 5, pp. 299–313, Jul. 2006.

[19] S. Osher and J. A. Sethian, "Fronts propagating with curvature-dependent speed: algorithms based on Hamilton-Jacobi formulations," *J. Comput. Phys.*, vol. 79, pp. 12–49, 1988.

[20] J. A. Sethian, "Theory , Algorithms , and Applications of Level Set Methods for Propagating Interfaces," *to Appear. Press. Acta Numer.*, 1995.

[21] J. A. Sethian, "Evolution, Implementation, and Application of Level Set and Fast Marching Methods for Advancing Fronts," *J. Comput. Phys.*, vol. 169, no. 2, pp. 503–555, May 2001.

[22] E. W. Dijkstra, "A Note on Two Problems in Connexion with Graphs," *Numer. Math.*, vol. 1, pp. 269–271, 1959.

[23] E. N. Marieb and K. Hoehn, *Human Anatomy & Physiology*, Eighth Edi. Pearson Learning Solutions, 2012.

[24] H. J. Johnson, M. M. Mccormick, and L. Ibañez, "The ITK Software Guide Book 1 : Introduction and Development Guidelines Fourth Edition Updated for ITK version 4 . 6," 2014.

[25] J. F. Canny, "A Computational Approach to Edge Detection," *IEEE Trans. Pattern Anal. Mach. Intell.*, vol. PAMI-8, no. 6, 1986.

[26] R. Deriche, "Fast algorithms for low-level vision," *IEEE Trans. Pattern Anal. Mach. Intell.*, vol. 12, no. 1, pp. 78–87, 1990.

[27] J. F. Canny, "Finding Edges and Lines in Images," Massachusetts Institute of Technology, 1983.

[28] R. Deriche, "Recursively Implementing the Gaussian and its Derivatives," INRIA Sophia-Antipolis, 1993.

[29] G. Farnebäck and C.-F. Westin, "Improving Deriche-style Recursive Gaussian Filters," *J. Math. Imaging Vis.*, vol. 26, no. 3, pp. 293–299, Nov. 2006.